

The Molecular Structure and Internal Rotation of Bis(pentamethylcyclopentadienyl)

Richard Blom

Department of Chemistry, University of Oslo, P.O. Box 1033 Blindern, N-0315 Oslo 3, Norway

Blom, R., 1988. The Molecular Structure and Internal Rotation of Bis(pentamethylcyclopentadienyl). – Acta Chem. Scand., Ser. A 42: 445–453.

The molecular structure, and in particular the potential energy as a function of torsional angle about the central C-C bond of bis(pentamethylcyclopentadienyl) (1,1',2,2',3,3',4,4',5,5'-decamethyl-bi-2,4-cyclopentadien-1-yl) has been studied by dynamic ^1H and ^{13}C NMR spectroscopy, molecular mechanics (MMP2), and gas-phase electron diffraction (GED). The observed temperature dependence of the NMR spectra has been interpreted on the basis of a model in which the molecule flips between two equally populated sites with torsional angles of $+\tau$ and $-\tau$ [$\tau \neq 0^\circ$ (*syn*) or 180° (*anti*)]. The activation barrier is found to be $\Delta H^\ddagger = 39.5(15)$ kJ mol $^{-1}$ and $\Delta S^\ddagger = -34(3)$ J K $^{-1}$ mol $^{-1}$. The MMP2 calculations indicate that the lowest barrier for the flip is for the path over $\tau = 180^\circ$ and that there are two energy minima between 0 and 180° , viz. at $\tau = 62^\circ$ (*syn-clinal*) and 152° (*anti-clinal*), with an energy difference of 1.25 kJ mol $^{-1}$ giving 41% *syn-clinal* at 115 °C. The barrier between the *syn-clinal* and *anti-clinal* forms is too low to affect the NMR spectra. The GED data are consistent with the presence of two conformers, but equally good fit can be obtained if one assumes only one conformer with a large amplitude torsional motion.

Dedicated to Professor Otto Bastiansen on his 70th birthday

Bis(pentamethylcyclopentadienyl), $(\text{C}_5\text{Me}_5)_2$ (Me = CH $_3$), has previously been reported as a by-product in the synthesis of pentamethylcyclopentadienyl tin^{1,2} and copper³ compounds. The reported preparation of $\text{Hg}(\text{C}_5\text{Me}_5)_2$ has met scepticism, since its ^1H NMR spectrum is identical with that of $(\text{C}_5\text{Me}_5)_2$, and the conclusion has been drawn that the compound originally postulated to be bis(pentamethylcyclopentadienyl) mercury in fact was bis(pentamethylcyclopentadienyl).^{1,4} The sample of $(\text{C}_5\text{Me}_5)_2$ used in the present study was obtained in high yield in an attempt to prepare $\text{Cd}(\text{C}_5\text{Me}_5)_2$. The related compounds bicyclopentyl and bicyclobutyl are mixtures of *gauche* and *anti* conformers in the gas phase.^{5,6} Introduction of methyl groups on the ring is expected to increase the inter-ring steric repulsions, which may alter the conformation significantly. Since bis(pentamethylcyclopentadienyl) is expected to be sterically strained and shows fluxional behaviour in the variable tem-

perature NMR spectra, we decided to carry out a full structure determination in order to clarify its conformation around the central C-C bond.

Experimental and data reduction

Synthesis. $(\text{C}_5\text{Me}_5)_2$ was prepared in a reaction between CdCl_2 and LiC_5Me_5 in THF at room temperature. LiC_5Me_5 was prepared by adding $\text{C}_5\text{Me}_5\text{H}$ (EGA, distilled) to a solution of LiMe in diethyl ether. The insoluble LiC_5Me_5 was removed by filtration and dried under vacuum. Anhydrous CdCl_2 (MERCK) was heated under reflux in THF for two hours. LiC_5Me_5 was then slowly added at room temperature. The solution was first light yellow, but after some minutes a gray precipitate appeared and after 4 h the yellow colour had disappeared leaving a clear solution with a dark reddish-gray precipitate (presumably $\text{Cd} + \text{LiCl}$). The precipitate was removed by filtration, and THF was distilled off under reduced

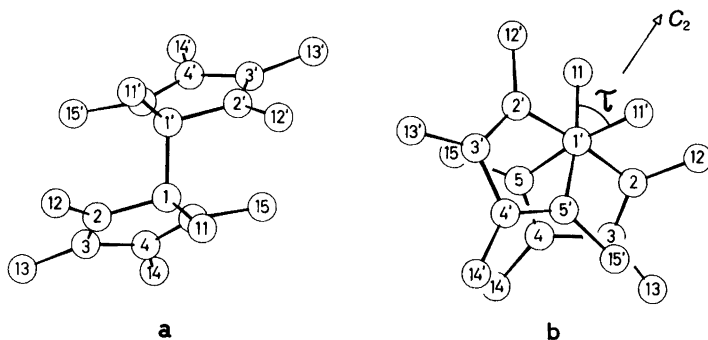


Fig. 1. The molecular model of C_2 symmetry considered in the gas-phase electron diffraction study of $(C_5Me_5)_2$. (a) Viewed along the C_2 axis, and (b) viewed along the $C1'-C1$ bond. The torsion angle, $\tau(C10-C1-C1'-C11')$, and numbering of the C-atoms are indicated. All H-atoms are omitted for clarity.

pressure. The white residue was dried under vacuum. The product was characterized as $(C_5Me_5)_2$ by 1H and ^{13}C NMR spectroscopy. The physical properties were identical to those previously reported.¹

NMR spectra. All 1H and ^{13}C spectra were recorded on a Varian XL-300 spectrometer oper-

ating at 299.943 MHz for 1H and 75.429 MHz for ^{13}C . The temperature measurements were performed by replacing the sample tube with a calibrated methanol thermometer. The error in the temperatures is estimated to be $\pm 1K$. Toluene- d_8 was used as solvent, and all shifts are reported with respect to toluene: the *meta* proton at δ 7.14 (1H) and C_1 at δ 138 (^{13}C). At low temperatures

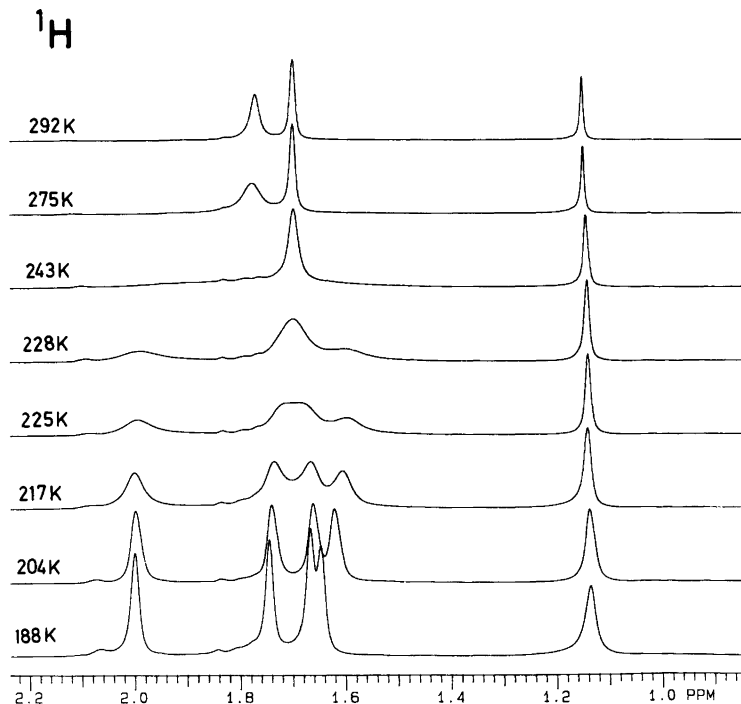


Fig. 2. 1H NMR spectra of $(C_5Me_5)_2$ in toluene- d_8 at different temperatures.

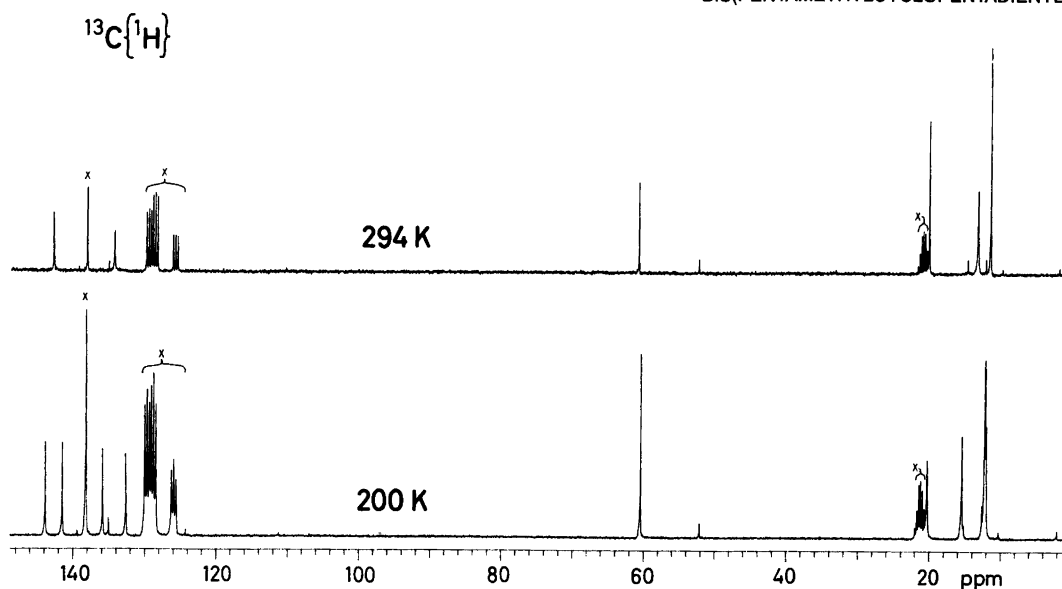


Fig. 3. Proton decoupled ^{13}C NMR spectra of $(\text{C}_5\text{Me}_5)_2$ in toluene- d_6 at 200 and 294 K. The solvent peaks are marked with x. The small peaks are due to impurities of $\text{C}_5\text{Me}_5\text{H}$.

the five peaks in the ^1H NMR spectra (see Fig. 2) indicate pairwise equivalence of the methyl groups of the two rings, which is consistent with C_2 molecular symmetry. The four peaks with large chemical shifts are assigned to the four

methyl groups attached to ring $\text{C}(\text{sp}^2)$, while the peak at δ 1.14 is assigned to the methyl group attached to ring $\text{C}(\text{sp}^3)$. At increased temperatures the four peaks with large chemical shifts coalesce to two peaks while the peak at δ 1.14 is

Table 1. Rate constants, k , and frequencies, ν , for the methyl groups attached to $\text{C}(\text{sp}^2)$ of the rings, obtained in the band-shape analysis of the exchange-broadened ^1H NMR spectra. Frequencies are in Hz relative to TMS.

T/K	ν_1	ν_2	ν_3	ν_4	k/sec^{-1}
188.2 ^a	600.0	523.6	500.1	494.3	—
201.5 ^a	599.9	522.4	498.8	487.6	—
203.7 ^a	599.6	522.2	498.6	486.4	—
209.7 ^a	599.8	521.9	498.6	484.2	—
217.5	600.5	522.1	498.5	481.3	23(2)
222.5	600.4	521.2	498.7	479.1	34(3)
224.9	599.2	521.0	498.5	478.3	41(4)
228.5	602.4	523.5	496.3	478.0	95(6)
233.6	601.4	522.1	497.7	474.8	133(9)
243.1	601.7 ^b	521.0	497.3	471.1 ^b	283(15)
259.2	602.3 ^b	525.4	492.8	464.5 ^b	1211(66)
275.5	605.4 ^b	532.9	486.3	460.2 ^b	3368(180)
291.5	608.2 ^b	542.4	477.9	455.8 ^b	6435(398)

^aAt these temperatures the frequencies are read directly from the spectra. ^bFixed values. The frequency differences, $\nu_1 - \nu_4$, were extrapolated from the values obtained at temperatures below 243.1 K. ^cThe rate constants have, in addition to the least-squares standard deviation, been given a fixed error of 5%.

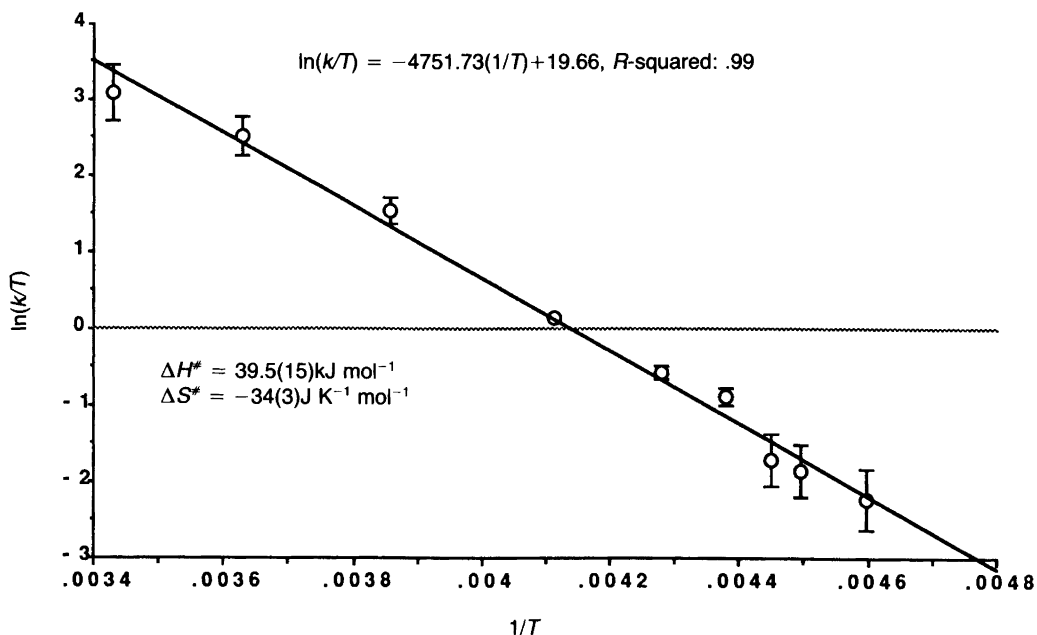


Fig. 4. The results from the exchange-broadened band-fit analysis. $\ln(k/T)$ plotted against $1/T$. k is the rate constant for the intramolecular flip from $\tau(\text{C11-C1-C1}'\text{-C11}') = \tau$ to $\tau(\text{C11-C1-C1}'\text{-C11}') = -\tau$.

unaffected. The spectra can only be understood if one assumes the equilibrium configuration of $(\text{C}_5\text{Me}_5)_2$ to be one of C_2 symmetry with $\tau(\text{C11-C1-C1}'\text{-C11}') \neq 0^\circ$ or 180° . The ^{13}C NMR spectra

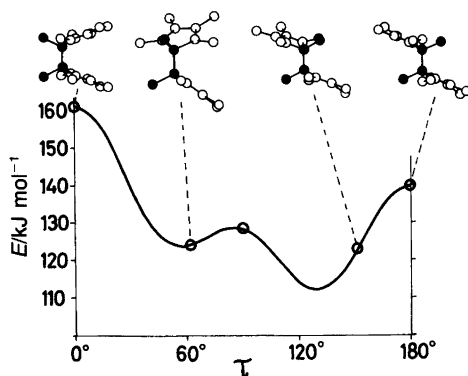


Fig. 5. MMP2 energies for different values of $\tau(\text{C11-C1-C1}'\text{-C11}')$ (points) with corresponding MMP2 molecular structures. The torsion angle, τ , is indicated by the dark atoms. The full curve is the least-squares fit of $E(\tau) = V_0 + V_1\cos\tau + V_2\cos2\tau + V_3\cos3\tau + V_4\cos4\tau$ to the MMP2 points: $E(\tau) = 125.6 + 10.4\cos\tau + 10.9\cos2\tau + 0.4\cos3\tau + 9.8\cos4\tau$.

at 200 and 295 K shown in Fig. 3, are consistent with this interpretation: At 200 K an assignment can be made on the basis of expectation values for the methyl carbon and $\text{C}(sp^2)$ chemical shifts:⁷ δ 11.6, 11.7, 11.8, 15.3 (C12-C15, C12'-C15'), δ 19.8 (C11, C11'), δ 60.0 (C1, C1') δ 132.0, 135.3, 140.8, 143.3 (C2-C5, C2'-C5'). At 294 K: δ 11.1, 12.8 (C12-C15, C12'-C15'), δ 19.6 (C11, C11'), δ 60.2 (C1, C1'), δ 133.6, 142.1 (C2-C5, C2'-C5').

An iterative dynamic NMR program for unsaturated exchange-broadened band shapes, DNMR5 (QCPE program no. 365), was used to calculate the rate constants for the intramolecular dynamic process, i.e. the flip from $\tau(\text{C11-C1-C1}'\text{-C11}') = \tau$ to $\tau(\text{C11-C1-C1}'\text{-C11}') = -\tau$. Only the ^1H NMR spectra have been used in these calculations over the exchange-broadened temperature range from 217 K to 292 K (see Fig. 1 and Table 1). The part of the spectrum from 450.0 to 700.0 Hz (δ 1.50 to δ 2.33) has been used in the band-fit analysis, while the T_2^* values are calculated from the half-width of the peak at δ 1.14. At temperatures below 233.6 K all four frequencies were refined along with the rate constant, k , and two baseline parameters, viz. the baseline increment

Table 2. The geometrical parameters and root-mean-square amplitudes of vibration (l -values) obtained for $(C_5Me_5)_2$ in the present gas-phase electron diffraction study (GED), and geometrical parameters from the MMP2 optimisations.

	GED		MMP2	
Parameters assumed to be equal for the two conformers:				
Distances/pm	r_a	l	r_e	
C1-C1'	156.5 ^a	5.8(6) ^c	156.5,155.8	
C1-C2	151.7(6)	5.4 ^c	152.9,153.0	
C2=C3	135.0(6)	4.3 ^c	135.2,135.2	
C3-C4	148(3)	5.2 ^c	145.6,145.5	
C1-C11	156(3)	5.8 ^c	154.0,154.2	
C2-C12	149.7(8)	5.6 ^c	150.8,150.6	
C-H	110.8(5)	7.6(4)	111.1,111.1	
C1...C3	234	7.6(4) ^d	240,240	
C2...C4	232	7.6 ^d	227,228	
C2...C5	238	7.6 ^d	228,231	
all C(Cp)...C'(Cp)	—	12–18(5)	—	
all C(Cp)...C'(Me)	—	27–31(12)	—	
all C(Me)...C'(Me)	—	14–20(4)	—	
Angles/°				
\angle C12-C2-C3	133(2)	—	124,124	
\angle C13-C3-C2	124(1)	—	125,126	
\angle C1-C2-C3	109.24 ^b	—	116,113	
\angle C-C-H	111(2)	—	111,111	
\angle C ₅ ,C1-C11	50(3)	—	52, 63	
Parameters assumed different for the two conformers:				
Conformer	<i>anti-clinal</i>	<i>syn-clinal</i>	<i>anti-clinal</i>	<i>syn-clinal</i>
τ (C11-C1-C1'-C11')	110–160°	64(8)°	152°	62°
\angle C ₅ ,C1-C1'	49–74°	63(3)°	63°	53°
Abundance/%	50(10)	50(10)	59	41

^aCould not be refined together with the other independent parameters and was therefore fixed at the MMP2 value. ^bFixed at the value found in cyclopentadiene. See Ref. 14. ^{c,d} l -values with identical index were refined with a constant difference. ^eThe values obtained for both conformers are listed in order to indicate the minor differences in these geometrical parameters for the two conformers.

and the baseline tilt. At higher temperatures the $\nu_1 - \nu_4$ frequency difference was linearly extrapolated from the low temperature results and kept fixed throughout the least-squares analysis, while ν_2 , ν_3 , k , and the two baseline parameters were refined. The results are listed in Table 1. The activation parameters, ΔH^\ddagger and ΔS^\ddagger , were obtained by least-squares fit of a straight line to the experimental points in an Eyring plot, as shown in Fig. 4. The estimated errors are 3σ , derived as explained by Sandström.⁸

Molecular mechanics calculations. All calculations were performed using Allingers MMP2 program in the MIMIC package.⁹ All atomic positions were optimized using different initial values of the torsion angle, τ (C11-C1-C1'-C11'). Two energy minima were obtained between 0 and 180° (see Fig. 5 and Table 2). The optimal energies when τ (C11-C1-C1'-C11') was fixed at 0°, 90° and 180° were also calculated in order to obtain some indication of the barrier heights for rotation around the C1-C1' bond.

Electron diffraction. The electron scattering pattern for $(C_5Me_5)_2$ was recorded on a Balzers Eldigraph KDG-2¹⁰ with nozzle and reservoir temperatures of 115(5)°C. A torus-shaped nozzle was used which permitted the scattering pattern to be recorded with a reservoir vapor pressure of about 1 Torr.¹¹ The electronic wavelength was calibrated against scattering patterns for benzene [$r(C-C) = 139.75$ pm] with an estimated standard deviation of 0.1%. The nozzle-to-plate distances were 497.97 and 248.03 mm. 4 plates at the long nozzle-to-plate distance and 3 at the short nozzle-to-plate distance were used. The data extended from $s = 15.0$ to 145.0 nm⁻¹ with $\Delta s = 1.25$ nm⁻¹ (long), and from $s = 85.0$ to 300.0 nm⁻¹ with $\Delta s = 2.5$ nm⁻¹ (short). Complex atomic scattering functions, $f(s)$, for H and C were calculated from an analytical representation of the atomic potential.¹² The data reduction was carried out by established procedures.¹³ A blackness correction of $1+0.03D+0.09D^2+0.03D^3$ was used. The molecular intensities were modified by multiplication with $s/|fC|/|fC|$. The backgrounds were computer drawn from a least-squares fit of the sum of a polynomial and a theoretical molecular intensity

curve to the experimental levelled intensity curve. The degree of the polynomial was 8 for both nozzle-to-plate distance sets. Individual curves for each set were averaged, but the average curves were not connected in the least-squares refinements.

The molecular models considered throughout the GED refinements are of C_2 symmetry with the C_2 axis perpendicular to the C1-C1' bond (see Fig. 1). Each C-CH₃ fragment has C_{3v} symmetry. The methyl groups attached to C(sp^3) are fixed in staggered positions, while the other methyl groups are fixed in positions with one CCCH torsion angle of 90° with two H atoms pointed away and one pointed towards the other ring. In addition, the following assumptions had to be made for each C_5Me_5 unit: the C_5C_5 skeleton has C_s symmetry with a planar C_5 ring with $\angle C1-C2-C3$ assumed equal to the corresponding angle in cyclopentadiene,¹⁴ the methyl carbon attached to the ring C(sp^3) and the C1-C1' bond lie in the C_s plane, the carbon atoms of the methyl groups attached to ring C(sp^2) lie in the ring plane and all C(sp^2)-Me bonds are equal, and all C-H bonds and CCH valence angles are equal. With these

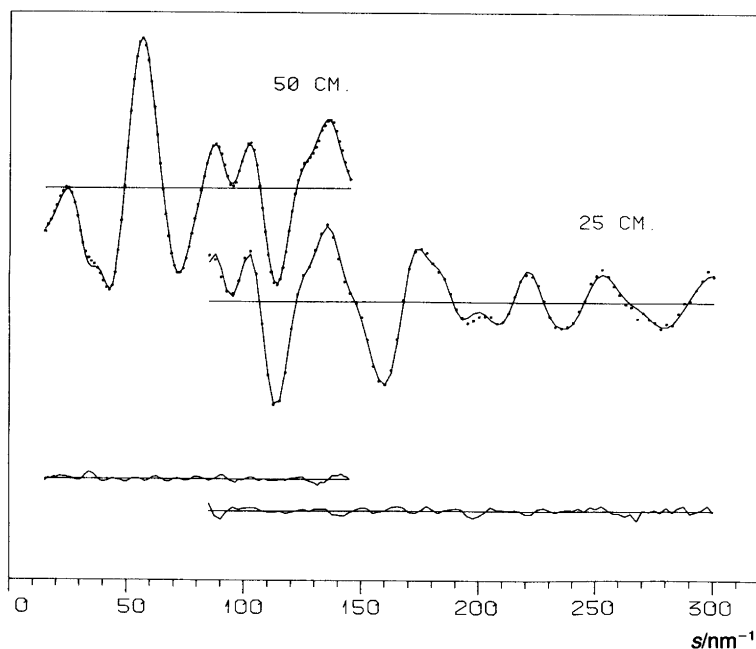
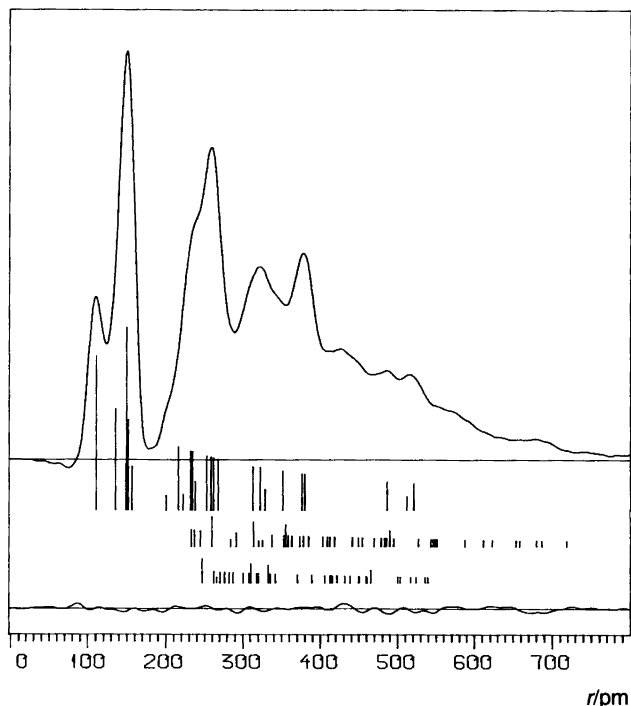


Fig. 6. Theoretical molecular intensity curves with experimental points for $(C_5Me_5)_2$. The difference between experimental and theoretical curves for the best model is drawn in the lower part of the figure.

Fig. 7. Experimental RD curve for $(C_5Me_5)_2$. The difference between the experimental and the theoretical curve calculated for the best model is drawn in the lower part of the figure. The most important distances are indicated with bars. Top: common for the two conformers; middle: inter-ring distances for the *anti-clinal* conformer; and bottom: inter-ring distances for the *syn-clinal* conformer. Artificial damping constant is 20 pm².



assumptions the molecular geometry is described by 13 geometrical parameters as noted in Table 2: six different C-C and the C-H bond distances, the angles between the ring plane and the $C(sp^3)$ -Me bond and the C1-C1' bond, denoted $\angle C_5, C1-C11$ and $\angle C_5, C1-C1'$, respectively, two exocyclic valence angles defining the positions of the methyl carbons attached to ring $C(sp^2)$, $\angle C3-C2-C12$ and $\angle C2-C3-C13$, respectively, the CCH valence angle, and the torsion angle $\tau(C11-C1-C1'-C11')$. In addition, 6 root-mean-square amplitudes of vibration (l -values) were refined as independent parameters as indicated in Table 2. The non-refined l -values were taken from a previous GED study of permethylated ferrocene.¹⁵ Most of the H...H distances are omitted in the calculations.

Since the MMP2 calculations indicated the presence of two conformers with an energy difference of only 1.25 kJ mol⁻¹, the possibility of two conformers was incorporated in the electron diffraction structure refinements. In these refinements all the independent parameters for the two conformers were assumed equal except the torsion angle, $\tau(C11-C1-C1'-C11')$, and the tip angle, $\angle C_5, C1-C1'$. These four angles and the mole fractions (α -values) of the two conformers were

refined along with the parameters described in the previous paragraph.

The theoretical molecular intensity curve calculated for the best two-conformer model with corresponding experimental points is drawn in Fig. 6. The corresponding experimental radial distribution (RD) curve is drawn in Fig. 7.

Results and discussion

The geometrical parameters and root-mean-square amplitudes of vibration (l -values) obtained in the GED study are listed in Table 2 along with the results from the MMP2 optimisations. The estimated errors noted in parentheses are the least-squares standard deviations multiplied by a factor of three in order to compensate for errors introduced by the many assumptions and data correlation, but they may still be too small. Numbering of the atoms and molecular models of the two conformers is shown in Fig. 1. In Fig. 5 the MMP2 energies are plotted against $\tau(C11-C1-C1'-C11')$. The curve is the least-squares fit of $E(\tau) = V_0 + V_1\cos\tau + V_2\cos2\tau + V_3\cos3\tau + V_4\cos4\tau$ to the MMP2 points.

The intramolecular rearrangement that gives

rise to the observed temperature dependence of the ^1H and ^{13}C NMR spectra must be interpreted to be a flip from $\tau(\text{C11-C1-C1}'\text{-C11}') = -\tau$ to $+\tau$ [$\tau \neq 0$ (*syn*) or 180° (*anti*)]. The MMP2 calculations indicate that the path over the barrier at 180° is the energetically favourable, and that the molecular structure in the transition state is of approximately C_{2v} symmetry. In principal, the MMP2 calculations only give the minimum value for the barrier height, in this case with the assumption that the barrier maximum is exactly that for $\tau(\text{C11-C1-C1}'\text{-C11}') = 180^\circ$. The MMP2 barrier height at 180° is $\Delta E(\text{MMP2}) = E(180^\circ) - E(152^\circ) = 16.4 \text{ kJ mol}^{-1}$. The activation parameters from the ^1H NMR band-shape analysis are $\Delta H^\ddagger = 39.5(15) \text{ kJ mol}^{-1}$ and $\Delta S^\ddagger = -34(3) \text{ J K}^{-1} \text{ mol}^{-1}$. With the assumption that the torsional frequency in the transition state is low, then $\Delta E(\text{MMP2}) \approx E_a$, the Arrhenius activation energy. The relationship between E_a and ΔH^\ddagger is $E_a = \Delta H^\ddagger + RT$, which gives $E_a = 42 \text{ kJ mol}^{-1}$ at 300 K, more than twice the $\Delta E(\text{MMP2})$ value. Conclusions based on a comparison of the two values should be drawn with care because of the unknown influence of solvent effects.

The MMP2 calculations indicate that the energy barriers are mainly due to inter-ring Me...Me repulsions. The four-fold barrier to the rotation around the C1-C1' bond can then be rationalized by considering the number of inter-ring Me...Me interactions much shorter than $2 \times$ the van der Waals radius for methyl groups of about 200 pm;¹⁶ for $\tau(\text{C11-C1-C1}'\text{-C11}') = 0^\circ$ there are three such interactions: C11...C11', C12...C15' and C15...C12', for $\tau(\text{C11-C1-C1}'\text{-C11}') = 90^\circ$ there are two: C11...C12' and C12...C11', and for $\tau(\text{C11-C1-C1}'\text{-C11}') = 180^\circ$ there are the two short interactions C12...C12' and C15...C15'. The full curve in Fig. 5 is a plot of the function $E(\tau) = 125.6 + 10.4\cos\tau + 10.9\cos 2\tau + 0.4\cos 3\tau + 9.8\cos 4\tau$. The $\cos 4\tau$ term determines the number of minima, while the $\cos 2\tau$ and $\cos \tau$ terms take care of the asymmetry of the rotation. The three-fold barrier term, $\cos 3\tau$, usually the predominant term for ethane-like derivatives, has only a minor contribution with a coefficient of 0.4.

Both the *syn-clinal* and *anti-clinal* conformers of C_2 symmetry have the same symmetry number as the transition state structure of C_{2v} symmetry. The negative sign of the activation entropy is then probably a consequence of the restricted

rotation of the methyl groups in the transition state due to inter-ring Me...Me interaction.

The GED results are quite uncertain. Different refinements gave very different values for the torsion angle, $\tau(\text{C11-C1-C1}'\text{-C11}')$, for the *anti-clinal* conformer. Values from 110 to 160° were obtained, with only insignificant differences in the R_2 factors¹⁷ and the other refined parameters, except $\angle \text{C5, C1-C1}'$ which varied from 49 to 73° . The torsion angle of the *syn-clinal* conformer was $64 \pm 8^\circ$ throughout the refinements, and the relative abundances of the two conformers were stable at $50 \pm 10\%$. From the GED investigations one may conclude that there is a quite rigid *syn-clinal* conformer with $\tau(\text{C11-C1-C1}'\text{-C11}') = 64(8)^\circ$, and an *anti-clinal* conformer with no well-defined torsion angle, which probably is a consequence of large-amplitude motion. The GED results cannot give an unambiguous answer to the question of whether there is a non-zero barrier between the two conformers or not. The latter would correspond to only one conformer which undergoes a large amplitude torsional motion. This structural problem is in fact at the edge of what is determinable by gas-phase electron diffraction methods.

The barrier between the *syn-clinal* and *anti-clinal* conformer is, according to the MMP2 calculations, at least 5.6 kJ mol^{-1} . This barrier is below what is detectable in a dynamic NMR study. No splitting or broadening of the five peaks in the ^1H NMR spectrum is observed at 188 K, which is consistent either with a low barrier between the two conformers or the presence of only one conformer.

Acknowledgements. I am grateful to Vigdis Bjerkelid and Aud Bouzga for performing the NMR experiments, to Hans V. Svelten for doing the GED experiments, and to Snefrid Gundersen for doing the photometer work.

References

1. Jutzi, P. and Kohl, F. *J. Organomet. Chem.* 164 (1979) 141.
2. Jutzi, P. and Hielscher, B. *Organometallics* 5 (1986) 1201.
3. Macomber, D. W. and Rausch, M. D. *J. Am. Chem. Soc.* 105 (1983) 5325.
4. Razavi, A., Rausch, M. D. and Alt, H. G. *J. Organomet. Chem.* 329 (1987) 281.

5. Bastiansen, O. and de Meijere, A. *Acta Chem. Scand.* 20 (1966) 516; Hagen, K., Hagen, G. and Trøtteberg, M. *Acta Chem. Scand.* 26 (1972) 3649.
6. de Meijere, A. *Acta Chem. Scand.* 20 (1966) 1093; Bastiansen, O. and de Meijere, A. *Angew. Chem.* 78 (1966) 142.
7. See e.g. Abraham, R. J. and Loftus, P. *Proton and Carbon-13 NMR Spectroscopy*, Wiley, Chichester 1978, p. 26.
8. Sandström, J. *Dynamic NMR Spectroscopy*, Academic Press, London 1982, p. 108.
9. Liljefors, T. *J. Mol. Graphics.* 1 (1983) 111; Allinger, N. L. *J. Am. Chem. Soc.* 99 (1977) 8127.
10. Zeil, W., Haase, J. and Wegmann, L. *Z. Instrumentenk.* 74 (1966) 84; Bastiansen, O., Graber, R. and Wegmann, L. *Balzers' High Vacuum Report* 25 (1969) 1.
11. Ashby, E. C., Fernholt, L., Haaland, A., Seip, R. and Scott Smith, R. S. *Acta Chem. Scand., Ser. A34* (1980) 213; *Annual Report of the Norwegian Electron Diffraction Group, Oslo*, Oslo 1980.
12. Strand, T. and Bonham, R. A. *J. Chem. Phys.* 40 (1964) 1686; Yates, A. C. *Comput. Phys. Commun.* 2 (1971) 175.
13. Andersen, B., Seip, H. M., Strand, T. and Stølevik, R. *Acta Chem. Scand.* 23 (1969) 3224.
14. Damiani, D., Terretti, L. and Gallinella, E. *Chem. Phys. Lett.* 37 (1976) 265.
15. Almenningen, A., Haaland, A., Samdal, S., Brunvoll, J., Robbins, J. L. and Smart, J. C. *J. Organomet. Chem.* 173 (1979) 293.
16. Pauling, L. *Nature of the Chemical Bond*, 3rd ed., Cornell University Press, New York 1960, p. 261.
17. $R_2 = \sqrt{[w(I_{\text{obs}} - I_{\text{calc}})^2/wI_{\text{obs}}^2]}$; Seip, H. M., Strand, T. G. and Stølevik, R. *Chem. Phys. Lett.* 3 (1969) 617.

Received February 2, 1988.